JOURNAL OF MATERIALS SCIENCE 27 (1992) 1626–1632

Theory and application of microindentation in studies of glide and cracking in single crystals of elemental and compound semiconductors

P. FELTHAM, R. BANERJEE
Department of Physics, Brunel University, Uxbridge, London UB8 3PH, UK

The microhardness of Si (MP 1688 K), GaP (1623 K), GaAs (1510 K) and InP (1327 K) single crystals was determined by indentation (Vicker's hardness, VHN) of low-index facets at loads of 5–100 g at 296–673 K, complementing earlier work on Ge and InSb. In the brittle range, extending up to about 0.35 T_{melt} (K), cracking occurred preferentially along the diagonals of the indentations, and was observed at all loads, with the possible exception of the lowest (5 g) in the case of InP at 289 K. At higher temperatures the relative orientations of crack and slip traces on the crystal surface, as observed by SEM, suggested that cracks nucleated preferentially at the slip-band intersection, as was also noted by Hirsch *et al.* (*Phil. Mag.* **3** (1985) 759) in GaAs above 600 K. As earlier in Ge, the VHN was found to depend on the load, L, as L^p, and on the indentation diameter, d, as d^n, with $p = \frac{1}{2}$ and $n = 2$, as required by the model of indentation plasticity of Banerjee and Feltham [4, 5], but higher p and n values were found if chipping at the indentation edges was evident. The effect was related to the resulting decrease in indentation diameter due to the work lost, through chipping, by the indenter. Above about 0.35 T_{melt} (K), relaxation of the dislocation structures entails a decrease of p and n; both parameters tend to zero as $T \rightarrow T_{melt}$. Shear and tensile stresses seem to co-operate in the process of plastic deformation, the role of normal stresses, acting across slip planes, predominating in the 'brittle' range.

1. Introduction

The almost universal choice of indentation as a method of studying plasticity in nominally brittle materials is largely due to the reduction in the propensity to cracking, which it affords as a result of the high compressive stresses below the tip of the diamond pyramid: these facilitate the application of loads to the indenter high enough to initiate local plastic flow, but too low to shatter the material. In the wake of the discovery of the transistor, indentation was widely used in work on the plasticity of crystals having diamond and associated sphalerite structures; a review covering the following two decades was published by Alexander and Haasen [1], later work was discussed by Feltham [2] and, more recently, by Hirsch [3].

Two papers dealing with the load-dependence (5–100 g) of the Vicker's hardness (VHN) of Ge [4] and InSb [5] crystals, indented at room temperature and in the range − 65–200 °C, respectively, refer to an appreciable load-effect. The VHN, which for an ideally plastic material of the Bingham type would not be expected to depend on the load, was found to be so only in InSb (MP 808 K) indented at temperatures exceeding about 0.35 T_{melt} (K), i.e. at 60, 110 and 200 °C. At − 65 °C, as with germanium at room temperature, the VHN was found to depend on the load as L^p, with p approximately equal to 0.43 for InSb and 0.50 for Ge. They explained the latter observations in terms of a specific mode of work-hardening in a deformation zone developing in the course of the penetration of the diamond, in which transport of the displaced material into the 'body' of the crystal is initiated by dislocations nucleating in the high-stress domains below the indenter. Some of the basic concepts embodied in the model subsequently found support in the dislocation arrangements observed by TEM [6] near indentations (100 g) made in silicon at room temperature.

More comprehensive pictures of the deformation structures emerged in the 1980s and in the present decade [7–15], particularly as a result of the application of SEM and high-resolution EM techniques to semiconductor materials used as substrates and devices. Of these, of most direct relevance to the present paper is the analysis of the indentation plasticity of GaAs, indented on {1 1 1} faces at 25–350 °C [7] and later publications e.g. on the structure [8–11] and mobility [12, 13] of dislocation in GaAs and other semiconductor crystals.

The main object of this work is to extend our earlier studies on the load-dependence of the VHN of germanium and indium antimonide [4, 5] to silicon and gallium arsenide, as well as to gallium and indium phosphides, with particular reference to combinations

0022–2461

of temperatures and indentation loads at which indentation creep is negligible. Adherence to this boundary condition was expected to facilitate an examination of the scope of our model [4] relating to the load-dependence of the VHN, in the light of the results. The crystallographic anisotropy of the VHN, discussed by Hirsch *et al.* [7] with reference to GaAs, and the dependence of the VHN on dopant types and levels [13] and, in the case of compound semiconductors, on the polarity of the indented face, insofar as they are determinants of the magnitude rather than the load-dependence of the VHN, are not examined here.

2. Experimental methods

Silicon (N-type, Sb-doped), gallium arsenide (N), gallium phosphide (P) and indium phosphide (P) single crystals, measuring $20 \times 2 \times 2$ mm, obtained from MCP Electronic Materials Ltd, Wokingham, UK, had the characteristics, supplied by the makers, given in Table I. All specimens were mechanically and then chemically polished; ~ 1 μm of the surface was removed in the latter stage. For indentation a Leitz microhardness tester was used up to 350 °C; a few indentations at somewhat higher temperatures were made with a carbide-steel indenter. In the latter case, specimens were pre-heated to slightly above the nominal test temperature in a vacuum furnace at about 10^{-4} torr before transfer to the indenter hot stage. Surface oxidation was, in general, found to be minimal. Indentations were made with loads of 5, 10, 15, 25, 50 and 100 g; a few tests with higher loads led, in general, to severe chipping. As in the case of germanium [4], the separation between adjacent indentations was always greater than 50 μm. For each combination of load and temperature, five indentations were usually made; the under-load period was standardized at 25 s. Indentation creep, as manifest by a significant decline in the VHN with increasing holding time of the indenter under load, was observed only at the highest loads (100 g), at temperatures well inside the region of the strong temperature dependence of the VHN (Fig. 1). Creep was negligible under all conditions for which values obtained for the VHN were correlated with other experimental parameters.

3. Results

The principal results, relating to the dependence of the VHN on temperature, load and indentation diameter,

TABLE I Characteristics of experimental materials

Material	Si	GaP	GaAs	InP
Carrier concentration (cm^{-3})	1.4×10^{12}	10^{15}	10^{15}	3×10^{17}
Resistivity at RT (Ω cm)	300	1.9	–	–
Carrier mobility ($cm^2\ Volt^{-1}\ s^{-1}$)	1500	3	8500	–
Dislocation density $\times 10^{-3}$ (cm^{-2})	3	–	10	–
Indices of the 20×2 mm faces	(1 1 1)	(1 1 1)	(1 0 0)	(1 0 0)

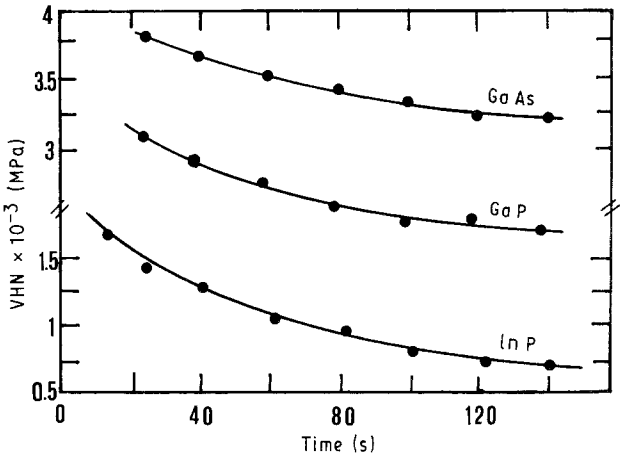

Figure 1 VHN as function of holding time of the indenter under load (100 g), for GaAs, GaP and InP indented at 350, 300 and 250 °C on (1 0 0), (1 1 1) and (1 0 0) facets, respectively. (For crystallographic detail of indentations on (1 0 0) and (1 1 1) for III–V crystals, see [3, 6].)

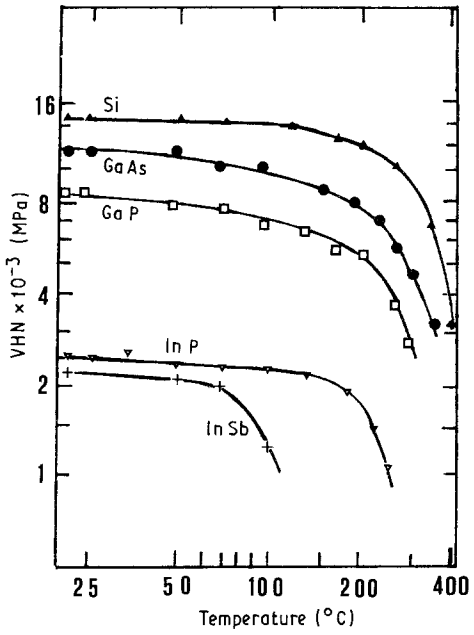

Figure 2 Temperature dependence of VHN, obtained with a 100 g load. Facets indented were (1 1 1), except for GaAs and InP, which were (1 0 0). Results for InSb taken from unpublished data related to [5]. ▲, Si; ●, GaAs; □, GaP; ▽, InP; +, InSb.

are shown in Figs 2–4; the first refers to a load of 100 g, the others to a temperature of 25 °C. The orientation dependence of the VHN of the silicon crystal, also at room temperature, is given in Fig. 5. (In conventional units of $kgf\ mm^{-2}$, the VHN may be obtained by multiplying the numbers on the ordinates by 100, e.g. '1' refers to a VHN of 100.)

For the combinations of load and temperature here used, complying with the requirement to avoid indentation creep, indentation was generally associated with observable cracking; chipping, which appeared to originate at the edges of the indentations, occurred at relatively high loads at all temperatures in this domain, silicon being particularly susceptible. Fig. 6 shows, as an example, chipping in the shape of four dimples in a gallium phosphide crystal indented on (1 1 1) at 65 °C with a load of 100 g. With lower loads,

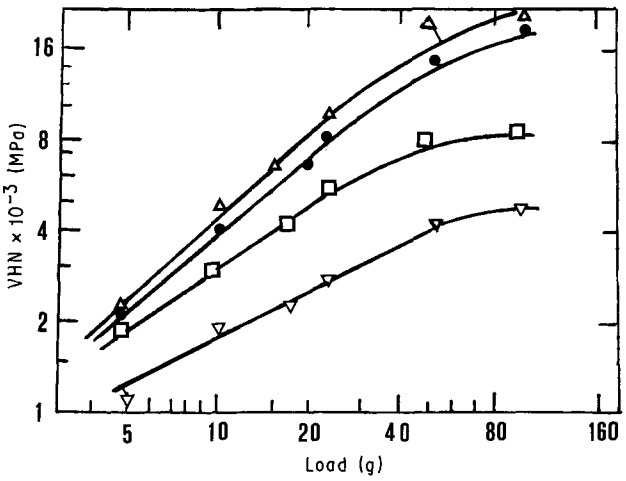

Figure 3 Dependence of VHN on indentation load at room temperature, in double logarithmic coordinates. Facets indented as in Fig. 2. ▲, Si; ●, GaAs; □, GaP; ▽, InP.

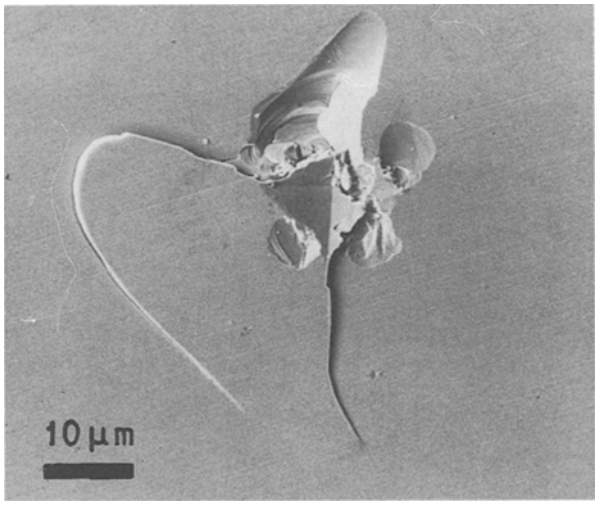

Figure 6 Cracking at indentation corners, and severe chipping, in gallium phosphide indented on (1 1 1) at 65 °C with a load of 100 g.

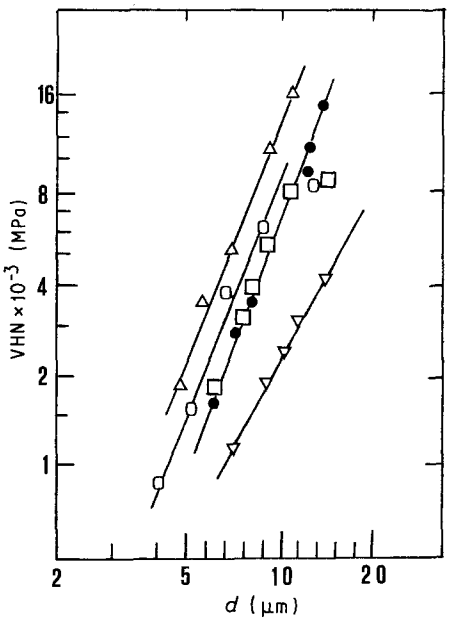

Figure 4 Dependence of VHN on indentation diameter at room temperature. Facets indented as in Fig. 2. Data for germanium (1 1 1) taken from [4]. Log/log coordinates. △, Si; ○, Ge; ●, GaAs; □, GaP; ▽, InP.

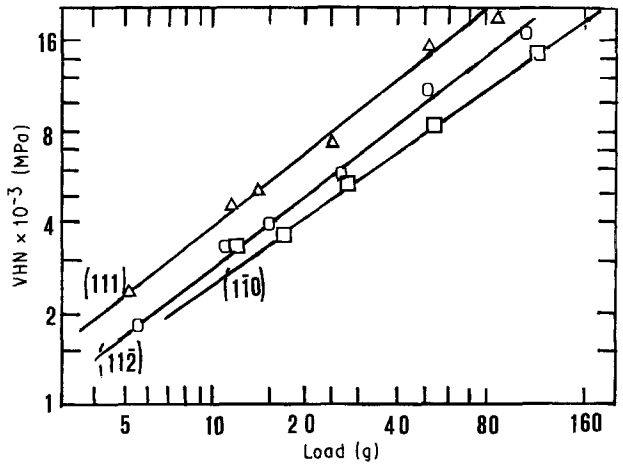

Figure 5 Load-dependence of VHN of silicon indented on three facets at room temperature. Log/log coordinates. △, (1 1 1); ○, (1 1 $\bar{2}$); □, (1 $\bar{1}$ 0).

chipping became less severe, e.g. three dimples or two on opposite edges of an indentation were observed. The dimple surfaces displayed a structure of tesselated terraces, characteristic of cleavage.

As with germanium crystals indented at room temperature [4], cracks observed in this low-temperature domain were commensurate in length with the indentation diameters, and appeared in general as extensions of the indentation diagonals, irrespective of the rotational symmetry of the crystal about the axis of the indenter. The crack length, c, which was in all cases taken as equal to the distance between the 'projected' apex of the indentation and the (sometimes not too well-defined) crack tip, correlated well with the relation

$$c \propto d - d_0, \tag{1}$$

where, again as with germanium at room temperature [4] $d_0 \cong 2$ μm, as found by rough extrapolation from data shown in Fig. 7. The relation suggests that cracking would not as a rule occur for loads for which $d < d_0$.

With temperature at which, under the present experimental conditions, the VHN becomes appreciably temperature-dependent, reflecting a relatively high mobility of glide dislocation, chipping no longer occurs, and extended cracks do not, in general appear on the crystal surface in alignment with the indentation diagonals. This is apparent, for example, from Figs 8 and 9 referring to gallium phosphide (0.35 T_m(K) = 295 °C) and indium phosphide (0.35 T_m = 191 °C), indented on (1 1 1) and (1 0 0) planes, respectively. With the 'sinking-in' type of indentation, as contrasted with those resulting in the formation of a lip at the surface, the release of compressive stresses under the indenter, as the latter is withdrawn, is accompanied by the transport of material by slip to the surface; the process, discussed by Hirsch *et al.* [7] in detail, favours the formation of cracks bisecting the angles between the operative slip systems. The traces of the latter, although barely apparent in Fig. 8a, are clearly evident at a higher temperature as an equilateral triangle (Fig. 8b). Similar features are apparent in the case of

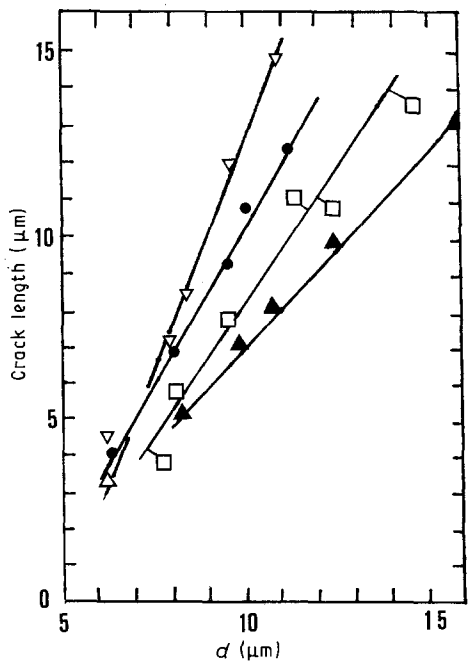

Figure 7 Mean lengths of crack traces as seen on crystal surfaces at room temperature on indentation with 5–100 g loads, as function of d. Length taken as distance from projected centre of indentation to crack tip. ▽, InP; ●, GaP; □, GaAs; ▲, Si.

indium phosphide (Fig. 9) indented on a (1 0 0) facet. Due to the four-fold rotation symmetry of the slip traces, the rosettes, indicated by arrows, now form a square pattern; cracks denoted by '1' approximately bisecting the angles of the square, and others (e.g. '2', which seems to have its origin at one side of the square), again appear to have formed in the stage of stress relaxation, on removing the indenter. The modes of cracking in the low-temperature 'brittle' state, in which slip markings were not resolved on the unetched crystal surfaces, thus appear to be fundamentally different from those characteristically associated with indentations made at higher temperatures, i.e. under conditions of relatively high dislocation mobilities [3].

4. Theoretical aspects and discussion

To facilitate an assessment of the scope of the theoretical interpretation of the load-dependence of the VHN in work-hardening and brittle crystals [4], with reference to the present results and the more recent literature, we shall briefly outline the basis of the model. A fundamental feature, shown schematically in Fig. 10, is the transport of material along active slip planes away from the indentation, as the indenter penetrates into the material. For clarity, two slip systems are shown separately; they facilitate slip sideways as well as in the direction of the indentation. An equivalent picture, specifically related to gallium arsenide indented on (1 1 1), is given by Hirsch *et al.* [3]. A sinking-in process is implied by Fig. 10: no protruding lip is indicated to have formed above the plastic zone surrounding the indentation. The envelope of 'dislocated' plastic material in a substantial volume around the indentation, which is known to grow in thickness with the depth of indentation [16], is in [4] assumed to have a volume proportional to d^3 where, during indentation, d represents the diagonal of the base of the pyramidal cavity. Proportionality between the length of the plastic zone, l, and the diameter, d, is thereby implied (Fig. 10).

On taking $L(d)$ to denote the instantaneous value of the load, as it increases from zero to its final value, L, one has for an increment of work done by the indenter

$$\delta W \propto L(d)\delta d \tag{2}$$

Further, it is assumed that the individual slip 'patches' are penny-shaped and of constant thickness, N being their number per unit volume of the plastic zone enveloping the cavity. The patches are taken to grow in the course of indentation in proportion to the length of the diagonals of the base of the pyramidal cavity, i.e. the ratio of the diameter of a patch to that of the instantaneous value of d remains constant. New patches, which form at the interface between the work-hardened and undeformed material, must have initial diameters equal to those of slip zones nucleated and grown in the earlier stages of the deformation. These scaling requirements imply uniformity of strain throughout the plastic mantle surrounding the indentation. On taking the energy of formation per unit area of the slip zones to be constant, the energy of deformation per unit volume of the mantle will be proportional to $Nd^3 d^2$, i.e. to Nd^5, so that one obtains for an increment of energy

$$\delta W \propto Nd^4\delta d \tag{3}$$

The Vicker's hardness number, defined as the full load, L, divided by the corresponding area of the base of

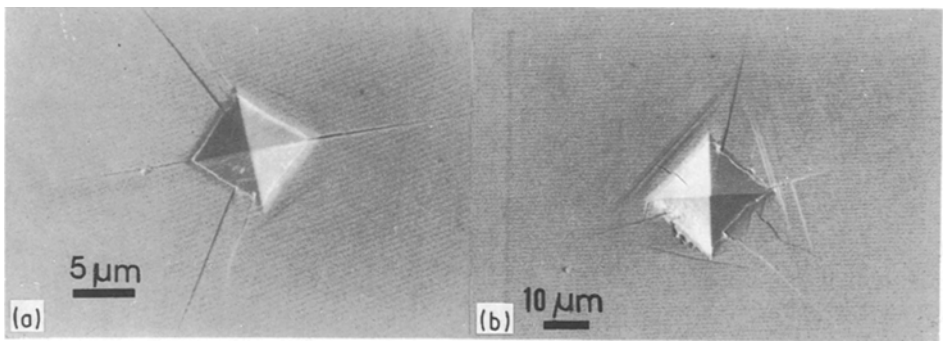

Figure 8 Gallium phosphide indented on (1 1 1) with a load of 100 g (a) at 300 °C, (b) at 350 °C. Cracks tend to bisect the angles of the rosette triangles. For discussion of high-temperature effects in GaAs see [7].

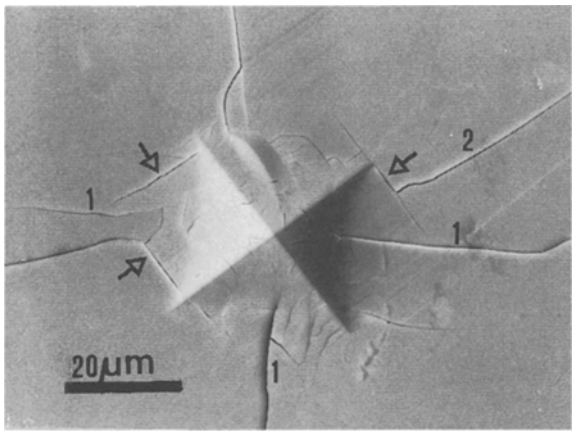

Figure 9 Indium phosphide indented (100 g) on (1 0 0) at 250 °C. (Note that $0.35\,T_{melt} = 191$ °C.) Arrows indicate cracks at intersection of slip planes with crystal surface, those denoted by '1' corresponding to the cracks shown in Fig. 8 on (1 1 1) surfaces. Crack denoted by '2' seems to have its counterpart in the one apparent in the brightest triangle of the indentation in Fig. 8b.

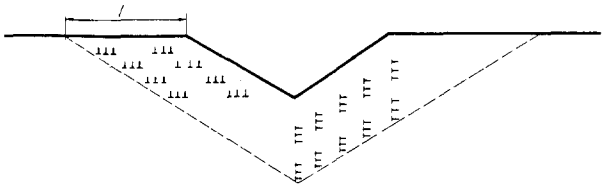

Figure 10 Two-dimensional, schematic, representation of the plastic patches as visualized in our model [4]. For the sake of clarity, only one of the two slip systems is shown on each side of the indentation.

the pyramidal cavity, $\frac{1}{2}d^2$, is

$$\mathrm{VHN} = 2L/d^2 \qquad (4)$$

where d now refers to the final diameter attained at 'full load'. Equation 4 yields, in conjunction with Equations 2 and 3, on elimination of δW between them,

$$\mathrm{VHN} \propto d^n \qquad n = 2 \qquad (5)$$

and as is readily verified,

$$\mathrm{VHN} \propto L^p \qquad p = \tfrac{1}{2} \qquad (6)$$

for the model. If the VHN is taken as a measure of the flow stress in compression of the material of the plastic envelope surrounding the indentation, and the corresponding strain due to the dislocations is assumed to be proportional to the area of slip associated with them, i.e. to Nd^2, with N constant, one notes that the coefficient of the work hardening, given by the stress/strain ratio, is independent of the diameter of the indentation, d, indicative of linear hardening. Without assuming specific values for n and p, consistency of Equations 4–6 requires that

$$p = n/(2 + n) \qquad \text{or} \qquad n = 2p/(1 - p) \qquad (7)$$

Experimentally determined values of n and p for Si, GaP, GaAs and InP crystals shown in Fig. 11 were obtained from the double-logarithmic representations given in Figs 3 and 4; in the case of n the linear sections of the curves, extending up to load values of approximately 40 g, were used. An n value of 2 for germanium, also indented with a load of 100 g at room temperature, was taken from Reference 4; the corresponding value of $p(=\frac{1}{2})$ was evaluated by means of Equation 7. The data pertaining to indium antimonide ($n = 1.5$, $p = 0.43$) were obtained by means of Equations 3–5, using $L \propto d^{3.5}$, as obtained [4] for indentations on (1 1 1) and other facets at loads of 1–100 g at − 65 °C. The arrows at the data points suggest that for indentation at room temperature, to which all other points refer, a shift of n and p to somewhat lower values is to be expected. The lines were drawn to pass through the point representing room temperature, for a hypothetical III–V compound close to melting would be expected to yield n, and hence p, equal to zero. It should be noted that, while for $2 \leqslant n \leqslant 3$, Equation 7 yields $0.5 \leqslant p \leqslant 0.6$, the upper limit (0.6) is exceeded for the crystals (Si, GaP and GaAs) with the highest melting points. These deviations seem to be a consequence of the pronounced chipping at the surface edges of the indentations, particularly at loads above about 40 g. A part of the work done by the indenter is not contributing to the shaping of the indentation proper; the latter is therefore smaller than would be the case without this loss of energy, and, on evaluating the VHN by means of Equation 4, an incorrect value is obtained.

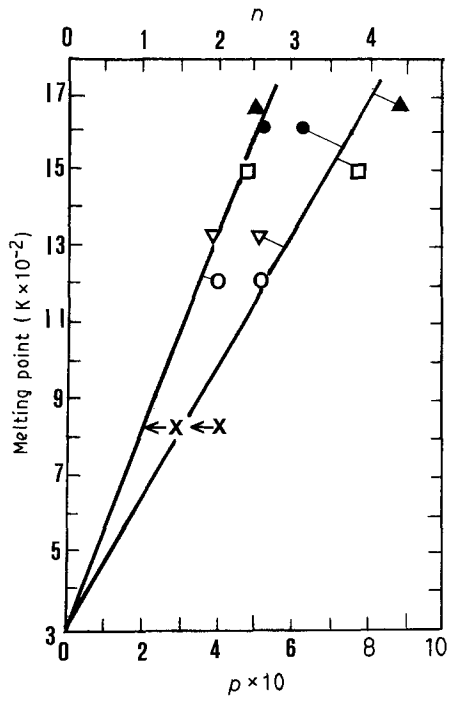

Figure 11 Indices n and p (Equations 5 and 6), with indentations as specified for Fig. 2, relate to room temperature, except those for InSb, denoted by x, which refer to − 65 °C and were evaluated, together with the p-value of germanium, from published data as described in the text. ▲, Si; ●, GaP; □, GaAs; ▽, InP; ○, Ge^x; ×, InSb*. (The upper line refers to 'n'.)

By contrast, n and p levels less than 2 and $\frac{1}{2}$, respectively, are indicated for indium antimonide (in Fig. 11). The discrepancy can be understood if it is considered that while for silicon and gallium arsenide, room temperature represents 0.18–0.20 T_{melt}(K), it is 0.26 at − 65 °C for indium antimonide. The relatively low n (1.5) and p (0.43) values thus suggest that some thermal recovery effects are beginning to take place,

resulting in a dislocation structure more relaxed than in crystals of higher melting points.

Concerning the characteristics of the dislocation patches, the high Peierls force has to be regarded as a basic determinant of their evolution and structure at all temperatures in the range here considered; thus, for example, the alignment of dislocations in silicon deformed at 420 °C along the ⟨1 1 0⟩ directions [17] provides a clear indication of its controlling influence on the deformation. Although deformation at these relatively high temperatures, at which crystallographic slip becomes manifest at the crystal surface (e.g. Figs 8 and 9, [7]), may not seem to have an immediate bearing on the mode of deformation occurring at lower temperatures, for which the patch concept was assumed to be relevant, it is instructive to consider some aspects of the transition from one to the other.

The yield stress of metals with a high Peierls force, e.g. B C C, at temperatures where no significant thermal recovery occurs, can be represented by the relation [18]

$$Q_0 \ln(\tau/\tau_0) = -mkT, \qquad m \approx 25 \qquad (8)$$

where τ_0 is its value as $T \to 0$ K, and Q_0 is the height of the energy barrier for $\tau/\tau_0 = e^{-1}$. On taking the VHN proportional to τ, Equation 8 is readily shown to represent the temperature dependence of the VHN (Fig. 2) in the high-temperature range quite well, e.g. down to about 135 °C in the case of silicon, and room temperature for indium antimonide. Extrapolation to 0 K yields VHN values about 2–4 times higher than the corresponding ones at the transitions to the brittle region; values of Q_0, starting with silicon, and proceeding in the order given in Fig. 2, were approximately 1.4, 1.2, 1.1, 0.7 and 0.3 eV. The rate determining process of the plastic deformation thus seems to be crystallographic slip [19], Peierls barriers being the main obstacles; bisection of the angle of intersection of traces of active slip planes, on the (1 1 1) indented surface, by straight cracks, e.g. as shown in Fig. 8, provides support for the view that these cracks nucleated in highly stressed domains of high dislocation density, close to the indenter, i.e. at intersections of active slip planes [7]. It seems that blockage of slip, e.g. due to the formation of Cottrell–Lomer barriers [7], but also as a result of the limited range of the stress field of the indenter, in combination with tensile stresses acting across the slip planes, facilitates cracking by a Griffith-type process. It may occur during indentation or on withdrawal of the indenter [7].

That slip takes place locally as a precursor to cracking at elevated temperatures was already observed in the 1970s by Tsunekawa and Weissmann [20], by X-ray topography of silicon subject to bending at temperatures between 500 and 800 °C. In notched crystals subjected to bending at 600 °C, a small micro-plastic zone was observed to develop at the tip of the notch prior to fracture.

In contrast, below the transition temperature (Fig. 2) the sequence glide-cracking appears to be reversed except, possibly, for rather small loads; we found evidence of corner cracking in germanium crystals indented at room temperature, with a load of 1 g [4]; in silicon, also indented at room temperature, with a load of 2 g, Eremenko and Nikitenko [21] found, in an early TEM study, Y-shaped cracking at the base of the indentation; the arms were about 1 μm long. The cracks were surrounded by a dense cluster of dislocations.

Later, Hill and Rowcliffe [6], also using TEM, observed cracks branching out from a nearly square hole at the base of a silicon crystal indented on a (1 1 1) plane with a 100 g load at room temperature. The shape suggests a relation to the shape of a cross-section of the indenter.

The pattern of dislocations surrounding the hole, as seen in a foil cut parallel to the plane of indentation, showed slip on (1 1 1) planes, i.e. parallel to the foil surface, as well as on the three remaining sets of planes of the slip tetrahedron, as was also found at higher temperatures. Allowing for the possibility of some relaxation of the dislocation structure during thinning of the foil, the characteristic features of the plastic deformation close to the indenter appear to be similar to those observed above the brittle–ductile transition temperature, and can be understood in terms illustrated in Fig. 10 [2]. They were later observed, for example, in gallium arsenide above the transition temperature by Hirsch *et al.* [7], and below it, in silicon, by Hill and Rowcliffe [6]. In the latter work, stereomicroscopy showed sets of concentric dislocation loops on planes parallel to that of the foil, lying at different depths of the crystal. The length of side of these patches was typically about 4 μm; the plastic zone extended up to 8 μm from the centre of the indentation. The loops consisted of long 30° and short 60° dislocation sections, and appear to be specific to low-temperature deformation for, as Hill and Rowcliffe [6] remark, at temperatures high enough to render the dislocations mobile in the internal stress field, 60° and screw dislocations were found to predominate. A description of the structures in terms of the patches postulated in our model [4] thus seems to be appropriate in both temperature regions. In the brittle range, possibly excepting the earliest stages of the indentation process, before slip zones of critical size have formed to facilitate nucleation of cracks by some Griffith-type mechanism, stored elastic energy seems to be released mainly by microcracking, in the course of which dislocations are generated and, after some movement into zones of lower deviatoric stresses, stopped. The cracking/slip process is then repeated as the indenter penetrates deeper into the crystal. If most of the microcracks are assumed to weld up following relaxation of the local stress through slip, the cracks could be regarded as catalysts of the low-temperature slip process. One could therefore expect that, unless significant indentation creep occurs, for example as in indium antimonide at or above room temperature (Fig. 11), or if the work of indentation is partly dissipated by chipping at the crystal surface, the indices, n and p, will be close to the respective values of 2 and $\frac{1}{2}$ given by our model (Equations 5 and 6). Smaller values of both indices would be expected at temperatures and indentation rates at which thermal recovery occurs during indentation, and higher values

would be expected if indenting is accompanied by chipping, as with Si, GaP and GaAs indented by a load of 100 g at room temperature (Figs 8 and 11). The pair of indices thus seem to be of potential diagnostic value in assessing the predilection of crystals, under specific conditions of indentation, either to flow or to chip; these results also indicate that the theory [4], particularly Equations 5 and 6, provides a basis for correlating thermal, crystallographic and mechanical features of low-temperature plasticity in semiconductor crystals.

References

1. H. ALEXANDER and P. HAASEN, *Solid State Phys.* **22** (1968) 27.
2. P. FELTHAM, *Abh. Ak. Wiss. DDR (Abt. Math., Naturwiss., Techn.)* **1N** (1978) 42.
3. P. B. HIRSCH, in "Dislocations and Properties of Real Materials", edited by M. H. Loretto (Institute of Metals, London, 1985) p. 343.
4. R. BANERJEE and P. FELTHAM, *J. Mater. Sci.* **9** (1974) 1478.
5. *Idem, ibid.* **11** (1976) 1171.
6. M. J. HILL and D. J. ROWCLIFFE, *ibid.* **9** (1974) 1569.
7. P. B. HIRSCH, P. PIROUZ, S. G. ROBERTS and P. D. WARREN, *Phil. Mag. B* **52** (1985) 759.
8. B. C. DE COOMAN and C. B. CARTER, *Phys. Status Solidi A* **112** (1989) 473.
9. *Idem., Phil. Mag. A* **60** (1989) 245.
10. N. D. THEODORE, B. C. DE COOMAN and C. B. CARTER, *Phys. Status Solidi A* **114** (1989) 105.
11. I. I. KHODOS, M. S. SHIKSAIDOV, I. I. SNIGHIREVA, A. P. UKSHAROVA and V. I. MIKHAILOVITCH, *ibid.* **114** (1989) 113.
12. J. VÖLKS, *Phil. Mag. A* **61** (1990) 233.
13. P. BROWN, J. RABIER and H. GAREM, *ibid.* **61** (1990) 619, 647 and 673.
14. P. B. HIRSCH, S. G. ROBERTS, J. SAMUEL and P. D. WARREN, in "Strength of Metals and Alloys", edited by P. O. Kettunen (Pergamon, Oxford, 1989) p. 1083.
15. V. I. BARBASHOV and T. V. RODZINA, *Phys. Status Solidi A* **115** (1989) K143.
16. R. WAGATSUMA, K. SUMINO, W. UCHIDA and S. YAMAMOTO, *J. Appl. Phys.* **42** (1971) 222.
17. A. OURMAZD, P. R. WILSHAW and G. R. BOOKER, *J. De Phys. (Paris)* **44** (1983) C4-51.
18. M. Z. BUTT, K. M. CHAUDHARY and P. FELTHAM, *J. Mater. Sci.* **18** (1983) 163.
19. P. B. HIRSCH and S. G. ROBERTS, *Phil. Mag. A.* **64** (1991) 55.
20. Y. TSUNEKAWA and S. WEISSMANN, *Metal Trans.* **5** (1974) 1585.
21. V. G. EREMENKO and V. I. NIKITENKO, *Phys. Status Solidi A* **14** (1972) 317.

Received 29 November 1990
and accepted 6 March 1991